Journal of Sound and Vibration 329 (2010) 4455–4465

Contents lists available at ScienceDirect

Journal of Sound and Vibration

journal homepage: www.elsevier.com/locate/jsvi

Multi-cracks detection of a beam-like structure based on the on-vehicle vibration signal and wavelet analysis

Khoa Viet Nguyen *, Hai Thanh Tran

Institute of Mechanics, Vietnam Academy of Sciences, Department of Technical Diagnoses, 264 Doi Can, Ba Dinh, Ha Noi, Viet Nam

ARTICLE INFO

Article history:
Received 26 March 2009
Received in revised form
7 May 2010
Accepted 7 May 2010
Handling Editor: H. Ouyang
Available online 2 June 2010

ABSTRACT

In this paper, a new method for detecting a multi-cracked beam-like structure subjected to a moving vehicle is presented. The crack model is adopted from fracture mechanics. The dynamic response of the bridge–vehicle system is measured directly from the moving vehicle. When moving along the structure, the moving vehicle causes small distortions in the dynamic response of the bridge–vehicle system at the crack locations. In general, these small distortions are difficult to detect visually. However, wavelet transform has recently emerged to be an effective method of detecting such small distortions. Large values (peaks) in the wavelet transform indicate the existence of the cracks. The locations of the cracks are pinpointed by positions of peaks of the wavelet transform and the velocity of the moving vehicle. Numerical results show that the method can detect cracks as small as 10% of the beam height. The proposed method is applicable for low velocity-movements while high velocity-movements are not recommended. The method presents an idea for measuring the vibration directly from the vehicle for crack detection problem in practice.

1. Introduction

The detection of cracks in mechanical systems and civil engineering structures has attracted many researchers in the last three decades as reviewed by Dimarogonas [1]. There are a large number of methods for crack detection that are based on the changes in the dynamic properties of the structure since cracks in structures may have a serious influence on their dynamic characteristics. The fact that a crack or local defect affects dynamic characteristics of structural members was known long ago [2]. According to the survey of Dimarogonas [1], in general, basic crack models exist, viz: the local flexibility model, the local bending moment or the equivalent reduced cross section model with magnitudes estimated by experimentation or by use of fracture mechanics. In practice, there are so many parameters that can be varied in vibration of cracked structures that it would be very difficult to present and compare results for all cases, for example modeling of the crack, coupling of flexural and longitudinal vibration. In order to apply test results considered assumptions and verifications for the crack models are required. The changes in stiffness, mass distribution and damping properties of the structures caused by cracks or flaws can alter the dynamic response of the damaged structures. However, there are various limitations in adopting this approach as the modification of the stress field induced by the crack declines with the distance from the crack [3–5]. Some other methods based on changes in modal parameters were also applied to the issue of damage detection. Pandey et al. [6] proposed the application of mode shape curvature in detecting damage. The reduction in cross

* Corresponding author. Tel.: +84 4 37624117.
E-mail address: nguyenvietkhoa_vc@yahoo.com (K.V. Nguyen).

0022-460X/$ - see front matter © 2010 Elsevier Ltd. All rights reserved.
doi:10.1016/j.jsv.2010.05.005

section caused by the damage tends to increase the curvature of the mode shapes in the vicinity of the damage. Verboven et al. [7,8] presented autonomous damage detection methods based on modal parameters. The changes in mode shapes of a slat track structure caused by the damage were auto-identified by using the frequency-domain maximum likelihood estimator method. Hu and Liang [9] proposed an integrated approach to detect cracks using the knowledge of changes in natural frequencies. In their work, the spring model and continuum damage model were combined to calculate crack locations and crack depths. Based on this approach, Patil and Maiti [10] developed a technique for detection of multiple cracks in slender beams which extends the scope of the method given in [9] from a single segment beam to multi-segment beams and eliminates the symbolic computation to determine the uncracked beam mode shapes. Damage assessment of multiple cracked beams was also studied by Ruotolo and Surace [11] using finite element model of the structure and genetic algorithms. In practice, a crack may not be only open or closed at all times, but it can open and close regularly depending on loading conditions on the cracked structure (residual loads, body weight of a structure, etc.), and the vibration effect. This crack type was termed a "breathing crack" and was discussed by Chondros et al. [12]. The dynamic response to harmonic excitation of a beam with several breathing cracks was analyzed by Ruotolo and Surace [13]. The authors used the "harmonic balance" approach to demonstrate that the presence of breathing cracks in a beam results in nonlinear dynamic behavior of the beam.

In the last decade, the wavelet transform has been shown as an efficient tool for signal processing due to its flexibility and precision in time and frequency resolution. Lu and Hsu [14] presented a wavelet based method for detection of structural damage. The minor localized damage induced significant changes of the wavelet coefficients at the location of the damage. Hong et al. [15] investigated the effectiveness of the continuous wavelet transform (CWT) in terms of its capability to estimate the Lipschitz exponent. In their study, the magnitude of the Lipschitz exponent was used as an indicator of the extent of damage when studying bending mode shapes of a cracked beam. A double-cracked beam was studied by Loutridis et al. [16]. The positions of the cracks were detected by the sudden changes in the spatial variation of the CWT. Poudel et al. [17] presented a wavelet-based method to localize damage in cantilever and simply supported beams using static deflection. In their experiments, the static deflections were obtained by processing digital photographs of the beams. Recently, Castro et al. [18,19] presented a wavelet based method for defect identification in rods subject to free and forced vibration. The existence and the location of the damage caused by local changes in density or stiffness of the rods, were detected by applying wavelet transform. The author of this paper and his co-author [20] presented a method for remote monitoring the cracked structure using the breathing crack phenomenon and wavelet transform. In this study, the crack was detected by analyzing the discontinuity of the dynamic response obtained from only one measurement point.

The analysis of continuous elastic systems subjected to moving subsystems has been a topic of interest for well over a century. Especially in bridge engineering many applications have been developed from the study of this subject. Parhi and Behera [21] presented an analytical method along with experimental verification to investigate the vibration behavior of a cracked beam under a moving mass. The Runge–Kutta method was used to solve the differential equations involved in analyzing the dynamic deflection of a cantilever beam. Piombo et al. [22] calculated the vehicle–bridge interaction system by considering it as a three-span orthotropic plate subject to a seven degrees-of-freedom multi-body system with linear suspensions and tires flexibility. Mahmoud and Abouzaid [23] presented iterative methods for the effect of single transverse cracks on the dynamic behavior of simply supported and cantilever undamped Euler–Bernoulli beams subject to a moving mass. According to this study the effect of the inertia force due to the moving mass is qualitatively similar, as well as additive, to the effect of the crack. Lee et al. [24] proposed a procedure for identification of the operational modal properties and the assessment of damage locations and their associated severities. The damage assessment was carried out based on the estimated modal parameters using the neural networks technique. Bilello and Bergman [25] studied damaged beams under a moving load. The damages were modeled by rotational springs whose compliance was evaluated using linear elastic fracture mechanics. Recently, Zhu and Law [26] successfully used CWT for crack detection by analyzing the operational deflection time history of a bridge subject to a moving vehicular load. Most of the current methods apply dynamic responses obtained from points on the bridge for crack detection.

The aim of this study is to extend the state-of-art of structural damage detection for bridges by presenting the wavelet based technique for the investigation of the dynamic response of a cracked beam-like bridge measured directly from the moving vehicle. It is a novel and simple method since it uses the dynamic response measured directly from the moving vehicle instead of responses measured on the bridge so that there is no need to set up measurements on the bridge. The theoretical model of a beam-like bridge with cracks and wavelet transform are presented. Numerical calculation is carried out to study the efficiency of the proposed technique.

2. Vibration of a beam-like structure under moving vehicle

2.1. Intact beam

We begin by considering the bridge–vehicle system shown in Fig. 1. In this study the half-vehicle model is adopted. The crack is assumed to be open all the time for the purpose of simplification. The bridge deck is modeled approximately as an Euler–Bernoulli beam. The surface unevenness of the bridge is disregarded and the tyres are assumed to be always in

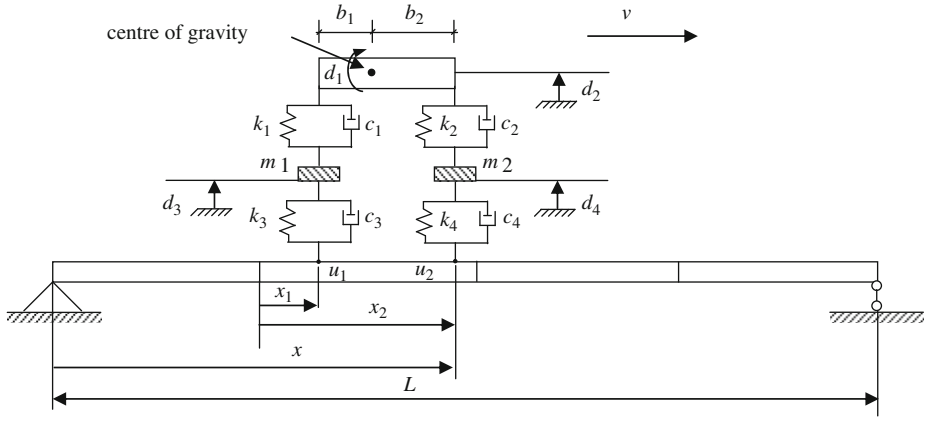

Fig. 1. A beam-like bridge under moving vehicle.

contact with the supported beam. Under these assumptions and based on [27,28] the governing equation of motion for the bridge–vehicle system can be derived as follows:

$$\begin{bmatrix} I_0 & 0 & 0 & 0 \\ 0 & m_0 & 0 & 0 \\ 0 & 0 & m_1 & 0 \\ 0 & 0 & 0 & m_2 \end{bmatrix} \begin{Bmatrix} \ddot{d}_1 \\ \ddot{d}_2 \\ \ddot{d}_3 \\ \ddot{d}_4 \end{Bmatrix} + \begin{bmatrix} b_1^2c_1+b_2^2c_2 & b_1c_1-b_2c_2 & -b_1c_1 & b_2c_2 \\ b_1c_1-b_2c_2 & c_1+c_2 & -c_1 & -c_2 \\ -b_1c & -c_1 & c_1+c_3 & 0 \\ b_2c_2 & -c_2 & 0 & c_2+c_4 \end{bmatrix} \begin{Bmatrix} \dot{d}_1 \\ \dot{d}_2 \\ \dot{d}_3 \\ \dot{d}_4 \end{Bmatrix} + \begin{bmatrix} k_1b_1^2+k_2b_2^2 & k_1b_1-k_2b_2 & -k_1b_1 & k_2b_2 \\ k_1b_1-k_2b_2 & k_1+k_2 & -k_1 & -k_2 \\ -k_1b_1 & -k_1 & k_1+k_3 & 0 \\ k_2b_2 & -k_2 & 0 & k_2+k_4 \end{bmatrix} \begin{Bmatrix} d_1 \\ d_2 \\ d_3 \\ d_4 \end{Bmatrix} = \begin{Bmatrix} 0 \\ 0 \\ k_3u_1+c_3\dot{u}_1 \\ k_4u_2+c_4\dot{u}_2 \end{Bmatrix} \tag{1}$$

$$[M]\{\ddot{d}\}+[C]\{\dot{d}\}+[K]\{d\}=[N_1]^Tf_1+[N_2]^Tf_2 \tag{2}$$

where

$$f_1=-m_1g-m_1\ddot{d}_3-\frac{m_0gb_2}{b_1+b_2}-\frac{I_0\ddot{d}_1+m_0b_2\ddot{d}_2}{b_1+b_2} \tag{3}$$

$$f_2=-m_2g-m_2\ddot{d}_4-\frac{m_0gb_1}{b_1+b_2}-\frac{I_0\ddot{d}_1+m_0b_1\ddot{d}_2}{b_1+b_2} \tag{4}$$

Here I_0, b_1, b_2, m_0, m_1, m_2, k_1, k_2, k_3, k_4, c_1, c_2, c_3, c_4 are vehicle parameters as shown in Fig. 1; d_1, d_2, d_3, d_4 denote the vehicle degrees of freedom; v is the vehicle velocity; u_1, u_2 are the vertical displacements of the contact points and equal to the vertical displacement of the beam at the contact positions; $[M]$, $[C]$ and $[K]$ are structural mass, damping and stiffness matrices; f_1 and f_2 are the interaction forces acting on the beam for contact points 1 and 2; g is gravitational acceleration; $[N]^T$ is the transposition of the shape functions at the position x of the interaction force; d is the nodal displacement of the beam. The displacement of the beam u at the arbitrary position x can be obtained from the shape functions $[N]$ and the nodal displacement d as [28]

$$u=[N]\{d\} \tag{5}$$

The shape function of an element can be obtained as

$$[N]=[N_1 \quad N_2 \quad N_3 \quad N_4] \tag{6}$$

where

$$\begin{aligned} N_1&=1-3\left(\frac{x}{l}\right)^2+2\left(\frac{x}{l}\right)^3, \quad N_2=x\left(\frac{x}{l}-1\right)^2, \\ N_3&=3\left(\frac{x}{l}\right)^2-2\left(\frac{x}{l}\right)^3, \quad N_4=x\left[\left(\frac{x}{l}\right)^2-\frac{x}{l}\right] \end{aligned} \tag{7}$$

with l being the length of the element.

The time derivatives of u are

$$\dot{u}(x,t) = \frac{\partial u}{\partial x}\dot{x} + \frac{\partial u}{\partial t} \tag{8}$$

Because $[N]$ is a spatial function while d is time dependent, from (5) we have

$$\frac{\partial u}{\partial x} = [N]_x\{d\} \tag{9}$$

where the subscript x implies the differentiation with respect to x. Substituting (8) and (9) into Eqs. (1) and (2) yields:

$$\begin{bmatrix} [M] & \sum_{i=1}^{2}[N_i]^T f_{\theta i} & \sum_{i=1}^{2}[N_i]^T f_{yi} & m_1[N_1]^T & m_2[N_2]^T \\ [0] & I_0 & 0 & 0 & 0 \\ [0] & 0 & m_0 & 0 & 0 \\ [0] & 0 & 0 & m_1 & 0 \\ [0] & 0 & 0 & 0 & m_2 \end{bmatrix} \begin{pmatrix} \{\ddot{d}\} \\ \ddot{d}_1 \\ \ddot{d}_2 \\ \ddot{d}_3 \\ \ddot{d}_4 \end{pmatrix} + \begin{bmatrix} [C] & \{0\} & \{0\} & \{0\} & \{0\} \\ [0] & b_1^2c_1+b_2^2c_2 & b_1c_1-b_2c_2 & -b_1c_1 & b_2c_2 \\ [0] & b_1c_1-b_2c_2 & c_1+c_2 & -c_1 & -c_2 \\ -c_3[N_1] & -b_1c_1 & -c_1 & c_1+c_3 & 0 \\ -c_4[N_2] & b_2c_2 & -c_2 & 0 & c_2+c_4 \end{bmatrix}$$

$$\times \begin{pmatrix} \{\dot{d}\} \\ \dot{d}_1 \\ \dot{d}_2 \\ \dot{d}_3 \\ \dot{d}_4 \end{pmatrix} + \begin{bmatrix} [K] & \{0\} & \{0\} & \{0\} & \{0\} \\ [0] & k_1b_1^2+k_2b_2^2 & k_1b_1-k_2b_2 & -k_1b_1 & -k_2b_2 \\ [0] & k_1b_1-k_2b_2 & k_1+k_2 & -k_1 & -k_2 \\ -k_3[N_1]-c_3[N_1]_x\dot{x}_1 & -k_1b_1 & -k_1 & k_1+k_3 & 0 \\ -k_4[N_2]-c_4[N_2]_x\dot{x}_2 & -k_2b_2 & -k_2 & 0 & k_2+k_4 \end{bmatrix} \begin{pmatrix} \{d\} \\ d_1 \\ d_2 \\ d_3 \\ d_4 \end{pmatrix} = \begin{pmatrix} \sum_{i=1}^{2}[N_i]^T\hat{f}_i \\ 0 \\ 0 \\ 0 \\ 0 \end{pmatrix} \tag{10}$$

where

$$f_{\theta 1} = \frac{1}{b_1+b_2}I_0, \quad f_{\theta 2} = -\frac{1}{b_1+b_2}I_0, \quad f_{y1} = \frac{b_2}{b_1+b_2}m_0, \quad f_{y2} = \frac{b_1}{b_1+b_2}m_0 \tag{11}$$

$$\hat{f}_1 = -\frac{b_2}{b_1+b_2}m_0g - m_1g, \quad \hat{f}_2 = -\frac{b_1}{b_1+b_2}m_0g - m_2g \tag{12}$$

2.2. Multi-cracked beam-like structure

Fig. 2 shows a uniform beam-like structure divided into Q elements with R cracks situated in R different elements. It is assumed that the cracks only affect the stiffness, while the mass and damping coefficient of the beam remain constant. According to the principle of Saint-Venant, the stress field is only affected in the region adjacent to the crack. Therefore, the element stiffness matrices of intact elements can be considered unchanged under certain limitations of element sizes, thus only the element stiffness matrices of cracked elements are changed. An element stiffness matrix of a cracked element can be obtained as follows [29]: Neglecting shear action, the strain energy of an element without a crack can be written as

$$W^{(o)} = \frac{1}{2EI}\left(M^2l + MPl^2 + \frac{P^2l^3}{3}\right) \tag{13}$$

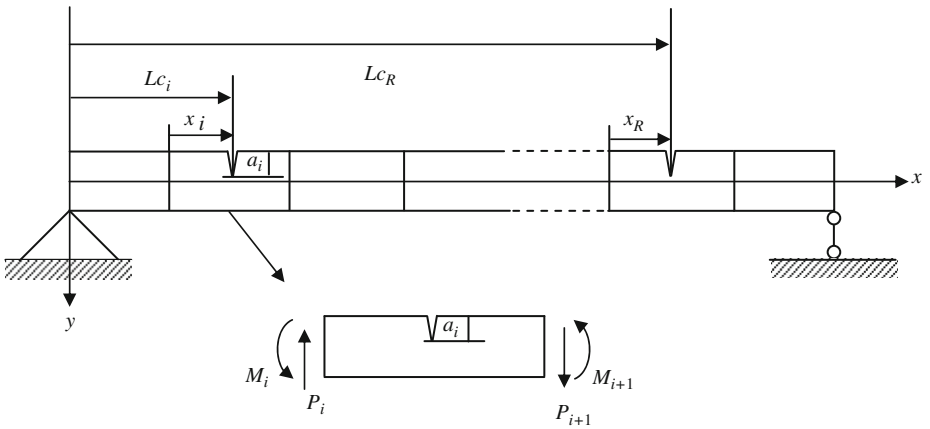

Fig. 2. Model of beam with R cracks.

where P and M are the shear and bending internal forces at the right node of the element (Fig. 2). The additional stress energy of a crack has been calculated from fracture mechanics and the flexibility coefficients are obtained by a stress intensity factor in the linear elastic range, using Castigliano's theorem. For a rectangular beam with the thickness h, the width b, and the additional energy due to the crack can be written as

$$W^{(1)} = b\int_0^a \left(\frac{(K_{\mathrm{I}}^2 + K_{\mathrm{II}}^2)}{E'} + \frac{(1+\nu)K_{\mathrm{III}}^2}{E}\right) \mathrm{d}a \tag{14}$$

where $E' = E$ for plane stress, $E' = E/1-\nu^2$ for plane strain and a is the crack depth, and K_{I}, K_{II}, K_{III} are stress intensity factor for opening type, sliding type and tearing type cracks, respectively.

Taking into account only bending, Eq. (14) leads to

$$W^{(1)} = b\int_0^a \frac{(K_{IM} + K_{IP})^2 + K_{IIP}^2}{E'} \mathrm{d}a \tag{15}$$

where

$$K_{IM} = \frac{6M\sqrt{\pi a}F_{\mathrm{I}}(s)}{bh^2}, \quad K_{IP} = \frac{3Pl\sqrt{\pi a}F_{\mathrm{I}}(s)}{bh^2}, \quad K_{IIP} = \frac{P\sqrt{\pi a}F_{\mathrm{II}}(s)}{bh} \tag{16}$$

$$F_{\mathrm{I}}(s) = \sqrt{\frac{2}{\pi s}tg\left(\frac{\pi s}{2}\right)}\frac{0.923 + 0.199[1-\sin(\pi s/2)]^4}{\cos(\pi s/2)} \tag{17}$$

$$F_{\mathrm{II}}(s) = (3s-2s^2)\frac{1.122 - 0.561s + 0.085s^2 + 0.18s^3}{\sqrt{1-s}} \tag{18}$$

The generic component of the flexibility matrix $\tilde{C}$ of the intact element can be calculated as

$$\tilde{c}_{ij}^{(o)} = \frac{\partial^2 W^{(o)}}{\partial P_i \partial P_j}, \quad i,j = 1,2, \quad P_1 = P, \quad P_2 = M \tag{19}$$

The additional flexibility coefficient is

$$\tilde{c}_{ij}^{(1)} = \frac{\partial^2 W^{(1)}}{\partial P_i \partial P_j}, \quad i,j = 1,2, \quad P_1 = P, \quad P_2 = M \tag{20}$$

Therefore, the total flexibility coefficient is

$$\tilde{c}_{ij} = \tilde{c}_{ij}^{(o)} + \tilde{c}_{ij}^{(1)} \tag{21}$$

From the equilibrium condition the following equation can be derived:

$$\begin{pmatrix} P_i & M_i & P_{i+1} & M_{i+1} \end{pmatrix}^T = [T]\begin{pmatrix} P_{i+1} & M_{i+1} \end{pmatrix}^T \tag{22}$$

where

$$[T] = \begin{pmatrix} -1 & -L & 1 & 0 \\ 0 & -1 & 0 & 1 \end{pmatrix}^T \tag{23}$$

By the principle of virtual work the stiffness matrix of the cracked element can be expressed as

$$[K]_c = [T]^T[\tilde{C}][T] \tag{24}$$

The stiffness matrix and mass matrix for an element without a crack can be obtained as

$$[K]_e = \frac{EI}{l^3}\begin{bmatrix} 12 & 6l & -12 & 6l \\ 6l & 4l^2 & -6l & 2l^2 \\ -12 & -6l & 12 & -6l \\ 6l & 2l^2 & -6l & 4l^2 \end{bmatrix} \tag{25}$$

$$[M]_e = \frac{ml}{420}\begin{bmatrix} 156 & 22l & 54 & -13l \\ 22l & 4l^2 & 13l & -3l^2 \\ 54 & 13l & 156 & -22l \\ -13l & -3l^2 & -22l & 4l^2 \end{bmatrix} \tag{26}$$

where I is the moment of inertia; E is Young's modulus; m and l are the mass and the length of the element, respectively.

Element mass matrices $[M]_e$ are assembled to form the global mass matrix $[M]$, while matrices $[K]_e$ and $[K]_c$ are assembled to form the global stiffness matrix $[K]$ of the cracked beam. Rayleigh damping in the form of $[C] = \alpha[M] + \beta[K]$ is

used for the beam. Where α and β are calculated as follows [28]:

$$\alpha = \frac{2\omega_1\omega_2(\xi_1\omega_2 - \xi_2\omega_1)}{\omega_2^2 - \omega_1^2}, \quad \beta = \frac{2(\xi_2\omega_2 - \xi_1\omega_1)}{\omega_2^2 - \omega_1^2} \tag{27}$$

Substituting global matrices [M], [C], and [K] of the cracked beam into Eq. (10) and solving this equation by the Newmark method, the dynamic responses of the vehicle and the beam will be obtained.

3. Wavelet transform

As the name suggests, wavelet transform analysis uses small wavelike functions known as "wavelets". A more accurate description is that a wavelet is a function which has local wavelike properties. Wavelets are used to transform a signal into another form of presentation in which the signal information is presented in a more useful form. Mathematically, the wavelet transform is a convolution of the wavelet function with the signal. Generally, wavelet transform transforms signals in time (or space) domain into time (or space)–frequency domain. This means that, via wavelet transform, a signal is presented in the frequency domain while the information in time (or space) domain is still retained. This is very useful for analysing short events or sudden changes contained in signals.

3.1. Continuous wavelet transform

The continuous wavelet transform is defined as follows [30]:

$$W(a,b) = \frac{1}{\sqrt{a}\int_{-\infty}^{+\infty} f(t)\psi^*\left(\frac{t-b}{a}\right)\mathrm{d}t} \tag{28}$$

where a is a real number called scale or dilation, b is a real number called position, $W(a,b)$ are wavelet coefficients at scale a and position b, $f(t)$ is input signal, $\psi(t-b/a)$ is wavelet function and $\psi^*(t-b/a)$ is complex conjugate of $\psi(t-b/a)$. In order to simplify the expression of the wavelet transform, denote $\psi_{a,b}(t) = (1/\sqrt{a})\psi^*(t-b/a)$, the wavelet transform (28) can be written

$$W(a,b) = \int_{-\infty}^{+\infty} f(t)\psi_{a,b}\,\mathrm{d}t \tag{29}$$

In order to be classified as a wavelet a function must satisfy the following mathematical criteria:

(1) A wavelet must have finite energy

$$E = \int_{-\infty}^{+\infty} |\psi(t)|^2\,\mathrm{d}t < \infty \tag{30}$$

(2) If $\hat{\psi}(\omega)$ is Fourier transform of $\psi(t)$, i.e.

$$\hat{\psi}(\omega) = \int_{-\infty}^{+\infty} \psi(t)e^{-i\omega t}\,\mathrm{d}t \tag{31}$$

then the following condition must be satisfied:

$$C_g = \int_0^{\infty} \frac{\left|\hat{\psi}(\omega)\right|^2}{\omega}\,\mathrm{d}\omega < \infty \tag{32}$$

This implies that the wavelet has no zero frequency component: $\hat{\psi}(0) = 0$,

$$\int_{-\infty}^{+\infty} \psi(t)e^{-j\omega t}\,\mathrm{d}t = 0 \quad \text{when } \omega = 0 \tag{33}$$

or in other words, the wavelet must have a zero mean

$$\int_{-\infty}^{+\infty} \psi(t)\,\mathrm{d}t = 0 \tag{34}$$

(3) An additional criterion is that, for complex wavelets, the Fourier transform must both be real and vanish for negative frequencies.

3.2. Inverse wavelet transform

Wavelet transform has its inverse transform:

$$f(t) = C_g^{-1}\int_{-\infty}^{+\infty}\int_{-\infty}^{+\infty} W(a,b)\psi_{a,b}\,\mathrm{d}b\,\frac{\mathrm{d}a}{a^2} \tag{35}$$

where

$$C_g = 2\pi \int_{-\infty}^{\infty} \frac{\left|\hat{\psi}(\xi)\right|^2}{|\xi|} \mathrm{d}\xi < \infty \tag{36}$$

Eq. (35) can be rewritten as follows:

$$f(t) = C_g^{-1} \int_{-\infty}^{+\infty} a^{-2} \left[\int_{-\infty}^{+\infty} W(a,b)\psi_{a,b}\, \mathrm{d}b \right] \mathrm{d}a \tag{37}$$

4. Numerical simulation and discussions

A numerical example of a beam with two cracks at locations of $Lc_1=L/3$ and $Lc_2=2L/3$ is analyzed. The crack depths of the two cracks are identical. Parameters of the beam are: Mass density is 7855 kg/m^3; modulus of elasticity $E=2.1\times10^{11}$ N/m^2; $L=50$ m; $b=1$ m; $h=2$ m. Modal damping ratios for all modes are equal to 0.01. Vehicle parameters are adopted from [31] as follows: $m_0=12{,}404$ kg; $m_1=m_2=725.4$ kg; $k_1=1{,}969{,}034$ N/m; $k_2=727{,}812$ N/m; $k_3=4{,}735{,}000$ N/m; $k_4=1{,}972{,}900$ N/m; $c_1=7181.8$ N s/m; $c_2=2189.6$ N s/m; $c_3=c_4=0$ N s/m; $I_0=172{,}160$ kg m^2; $b_1=b_2=3$ m. The displacement–time history of the moving vehicle is obtained to investigate the influence of the cracks. When the beam is cracked, there are distortions in the dynamic response of the vehicle at the crack locations. However, these local distortions are generally small and difficult to detect visually. Therefore, in this work the CWT, with its special properties, is applied for data processing. After trying several differing wavelet functions for signal processing, the wavelet function "Symlet" is chosen as the most suitable for this study.

In this section the influence of the cracks on the dynamic response of the vehicle moving with different velocities on the intact beam and the cracked beam is studied. Fig. 3 presents the dynamic responses of the vehicle moving at different velocities on the intact beam and the cracked beam with the crack depth of 50% of the beam height. As can be seen from this figure, considering a vehicle travelling at the same velocity, the dynamic response of the vehicle moving on the cracked beam is greater than that of the intact beam. However, no sign of local distortions caused by cracks can be seen in this figure. This is obviously true for the case of the intact beam (solid lines), but for the cracked beam (dotted lines) this means that the local distortions in the dynamic response of the vehicle caused by the cracks is extremely small.

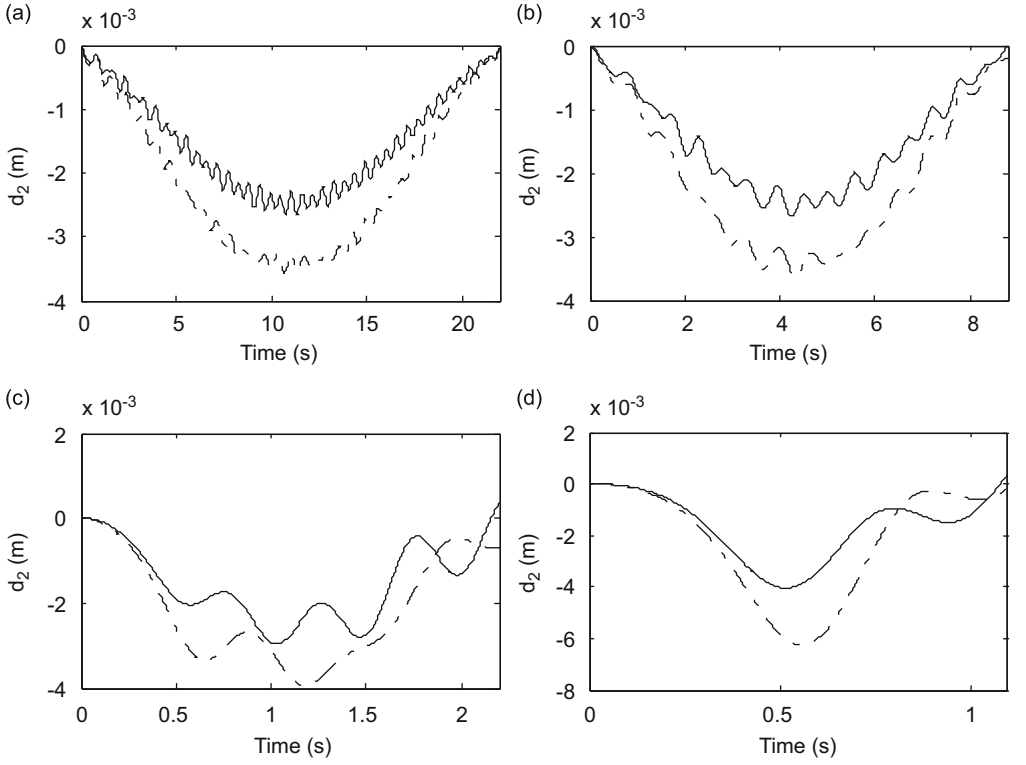

Fig. 3. Displacements of the vehicle moving on the beam with cracks (dotted lines) and without cracks (solid lines), with different velocities: (a) $v=2$ m/s, (b) $v=5$ m/s, (c) $v=20$ m/s, and (d) $v=40$ m/s.

4.1. Influence of the crack depth

In order to detect local distortions in the dynamic response of the vehicle due to the presence of cracks, the wavelet transform is applied. The velocity of the vehicle is v=2 m/s. Fig. 4 shows the wavelet transform of the vertical displacement of the vehicle. As can be seen in this graph, there are no significant peaks in the wavelet transform. However, when cracks are present, the wavelet transforms, using a scale of 50, clearly show four peaks at t=5.3, 8.3, 13.7, and 16.7 s (see Figs. 5–7). The peaks at t=5.3 and 8.3 s correspond to the moments when the first leg and the second leg of the vehicle pass by the location of $L/3$ of the beam, while the peaks at t=13.7 and 16.7 s correspond to that of $2L/3$. The peaks of the wavelet transforms explain that there are distortions in the dynamic response of the vehicle at moments when the two legs pass by the crack positions. This result implies that the cracks cause the distortions in the dynamic response of the vehicle at their locations, or in other words, the distortions in the dynamic response appear when the moving vehicle is passing by the crack locations. Therefore, the peaks in the wavelet transform indicate the existence of the cracks, and the positions of these cracks can be easily ascertained from the positions of the peaks and the velocity of the vehicle.

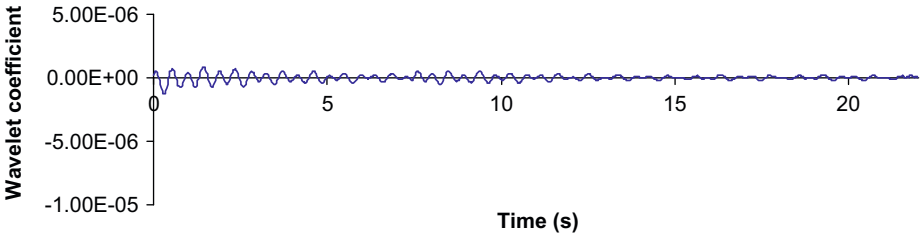

Fig. 4. Wavelet transform of $d_2(t)$. Crack depth is 0% and v=2 m/s.

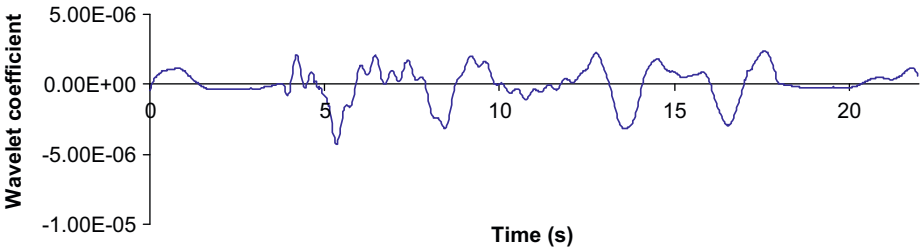

Fig. 5. Wavelet transform of $d_2(t)$. Crack depth is 10% and v=2 m/s.

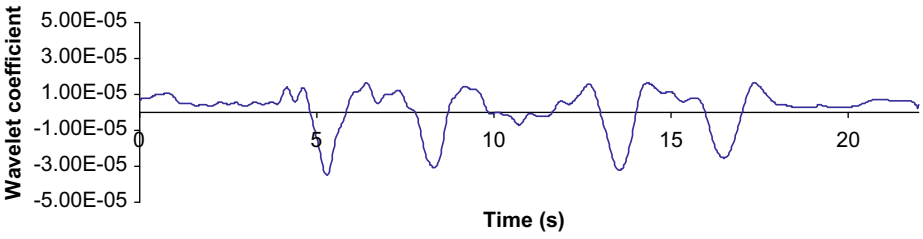

Fig. 6. Wavelet transform of $d_2(t)$. Crack depth is 30% and v=2 m/s.

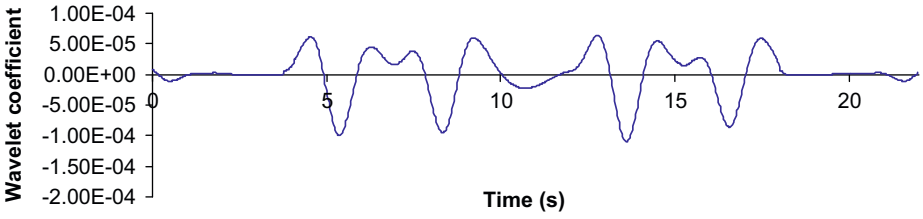

Fig. 7. Wavelet transform of $d_2(t)$. Crack depth is 50% and v=2 m/s.

As can be seen in Figs. 5–7, when the crack depth increases from 10% to 50%, the peaks at moments when the two legs pass by the position of the crack are more significant. This means that the larger the crack depth is the more consistent the proposed method for crack detection becomes.

4.2. Influence of the velocity of the moving vehicle

In this study, the influence of the velocity of the moving vehicle on the crack detection problem is also investigated. While cracks as small as 10% of the beam height can be detected when the vehicle is moving at low velocity as presented in the above section, they are very difficult to be revealed at high velocities. In case of high velocities, distortions caused by cracks can only be detected for various specific velocities and in respect of cracks with depths larger than or equal to 50%. Fig. 8 presents the wavelet transforms with scale 5 of the vertical displacements of the vehicle moving at the speed of 30 m/s on the cracked beam with the crack depth of 50%. In this figure, only two peaks, corresponding to the moments when the second leg passes by the cracks, are detected and the peak values are very small in comparison with the case of low velocity shown in Section 4.1. This means that it is much more difficult to detect the cracks when the vehicle velocity is high.

As can be seen in Fig. 8, the two significant peaks are sharper in comparison with the case of low velocity. As presented when the velocity is low, the significant peaks in wavelet transform occur at scale 50. But when the velocity is higher, the significant peaks appear at the smaller scale 5. According to the wavelet transform, this expresses that when the vehicle travels at low speed it causes low frequency (high scale) distortions in the dynamic response of the vehicle and when the vehicle travels at high speed it causes distortions with higher frequencies (low scale).

4.3. Influence of the noise

In order to simulate the polluted measurements, white noise is added to the calculated responses of the vehicle. The noisy response is calculated as following formula:

$$d_{2\text{noisy}} = d_2 + E_p N \sigma(d_2) \tag{38}$$

where d_2 is the vertical displacement of the vehicle body obtained from the numerical simulation. E_p is the noise level and N is a standard normal distribution vector with zero mean value and unit standard deviation. $d_{2\text{noisy}}$ is the noisy displacement, and $\sigma(d_2)$ is its standard deviation.

Fig. 9 show the wavelet transform of the noisy and unnoisy responses of the vehicle moving on the beam with the crack depth of 50% and the velocity of the vehicle at 2 m/s. In this case, the cracks can be detected with the noise level up to 6%.

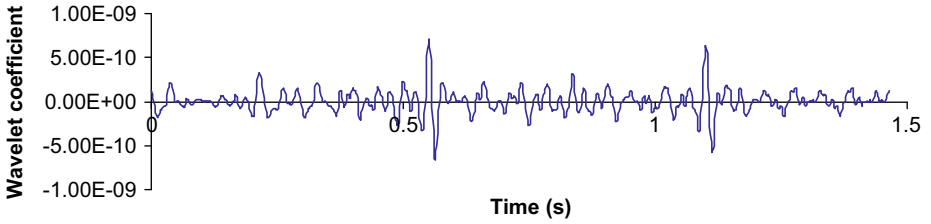

Fig. 8. Wavelet transform of $d_2(t)$. Velocity is 30 m/s and crack depth is 50%.

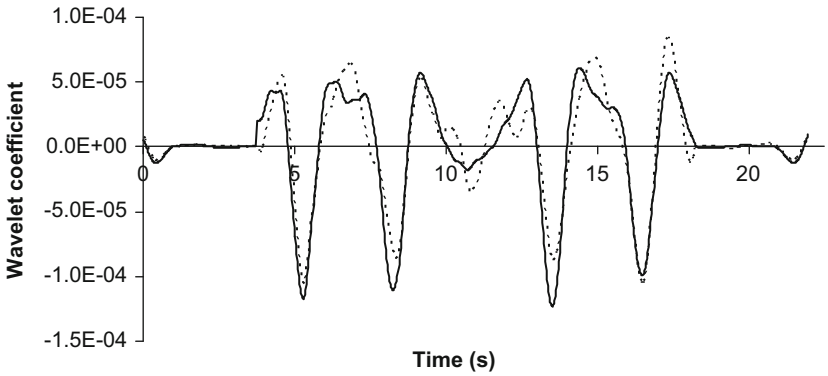

Fig. 9. Wavelet transform of dynamic responses of the vehicle, v=2 m/s. Solid line: 0% noise; dotted line: 6% noise.

5. Conclusions

A new technique for structural damage detection based on the wavelet transform of the dynamic response obtained from a moving vehicle is presented.

The existence of the cracks is detected by the large values (peaks) in the wavelet transform of the dynamic response. The positions of the cracks can be determined easily from the velocity of the vehicle and the locations of the peaks in the wavelet transform.

The advantage of the method is that it removes the need of choosing the positions of sensors on the deck of the bridge since the vibration data is measured directly from the moving vehicle. It is also a simple method because it uses only one vibration transducer attached to the vehicle. In addition, no information of the intact structure is needed for crack detection. From the results, the present method can be applied to detect small cracks with a depth of 10% of the beam height. This method is more sensitive than frequency based methods since the natural frequencies are almost constant for cracks up to a depth of 50% of the beam after which they slowly decrease [32,33].

From the investigation of the influence of the noise on the proposed method, it is concluded that the method can be applied for the case of non-polluted measurements as well as for the case of polluted measurements with the noise level up to 6%.

The proposed method can be applied efficiently with low vehicle speeds, while high speeds are not recommended.

To validate the method presented herein, experimental testing needs to be carried out at a future date.

Acknowledgements

This paper was sponsored by the Fulbright Scholar Program 2008–2009—Advanced Research and University Lecturing Awards in the United States.

References

[1] A.D. Dimarogonas, Vibration of cracked structures—a state of the art review, *Engineering Fracture Mechanics* 5 (1996) 831–857.
[2] T.G. Chondros, A.D. Dimarogonas, Identification of cracks in welded joints of complex structures, *Journal of Sound and Vibration* 69 (1980) 531–538.
[3] T.G. Chondros, A.D. Dimarogonas, Dynamic sensitivity of structures to cracks, *Journal of Vibration, Acoustics, Stress and Reliability in Design* 111 (1989) 251–256.
[4] T.G. Chondros, The continuous crack flexibility method for crack identification, *Fatigue & Fracture of Engineering Materials & Structures* 24 (2001) 643–650.
[5] D. Panteliou, T.G. Chondros, V.C. Argyrakis, A.D. Dimarogonas, Damping factor as an indicator of crack severity, *Journal of Sound and Vibration* 241 (2) (2001) 235–245.
[6] A.K. Pandey, M. Biswas, M.M. Samman, Damage detection from changes in curvature mode shapes, *Journal of Sound and Vibration* 145 (2) (1991) 321–332.
[7] P. Verboven, E. Parloo, P. Guillaume, M.V. Overmeire, Autonomous structural health monitoring – part I: modal parameter estimation and tracking, *Mechanical Systems and Signal Processing* 16 (4) (2002) 637–657.
[8] P. Verboven, E. Parloo, P. Guillaume, M.V. Overmeire, Autonomous structural health monitoring – part II: vibration-based in-operation damage assessment, *Mechanical Systems and Signal Processing* 16 (4) (2002) 659–675.
[9] J. Hu, R.Y. Liang, An integrated approach to detection of cracks using vibration characteristics, *Journal of the Franklin Institute* 330 (5) (1993) 841–853.
[10] D.P. Patil, S.K. Maiti, Detection of multiple cracks using frequency measurements, *Engineering Fracture Mechanics* 70 (2003) 1553–1572.
[11] R. Ruotolo, C. Surace, Damage assessment of multiple cracked beams: numerical results and experimental validation, *Journal of Sound and Vibration* 206 (4) (1997) 567–588.
[12] T.G. Chondros, A.D. Dimarogonas, J. Yao, Vibration of a Beam with a Breathing Crack, *Journal of Sound and Vibration* 239 (1) (2001) 57–67.
[13] N. Pugno, C. Surace, R. Ruotolo, Evaluation of the non-linear dynamic response to harmonic excitation of a beam with several breathing cracks, *Journal of Sound and Vibration* 235 (5) (2000) 749–762.
[14] C.J. Lu, Y.T. Hsu, Vibration analysis of an inhomogeneous string for damage detection by wavelet transform, *International Journal of Mechanical Science* 44 (2002) 745–754.
[15] J.-C. Hong, Y.Y. Kim, H.C. Lee, Y.W. Lee, Damage detection using the Lipschitz exponent estimated by the wavelet transform: applications to vibration modes of a beam, *International Journal of Solids and Structures* 39 (2002) 1803–1816.
[16] S. Loutridis, E. Douka, A. Trochidis, Crack identification in double-cracked beam using wavelet analysis, *Journal of Sound and Vibration* 277 (2004) 1025–1039.
[17] U.P. Poudel, G. Fu, J. Ye, Structural damage detection using digital video imaging technique and wavelet transformation, *Journal of Sound and Vibration* 286 (2005) 869–895.
[18] E. Castro, M.T. Garcia-Hernandez, A. Gallego, Damage detection in rods by means of the wavelet analysis of vibration: influence of the mode order, *Journal of Sound and Vibration* 296 (2006) 1028–1038.
[19] E. Castro, M.T. Garcia-Hernandez, A. Gallego, Defect identification in rods subject to forced vibration using the spatial wavelet transform, *Applied Acoustics* 68 (6) (2007) 699–715.
[20] K.V. Nguyen, O.A. Olatunbosun, A proposed method for fatigue crack detection and monitoring using the breathing crack phenomenon and wavelet analysis, *Journal of Mechanics of Materials and Structures* 2 (3) (2007) 400–420.
[21] D.R. Parhi, A.K. Behera, Dynamic deflection of a cracked beam with moving mass, *Proceedings of the Institution of Mechanical Engineers* 211 Part C (1997) 77–87.
[22] B.A.D. Piombo, A. Fasana, S. Marchesiello, M. Ruzzene, Modelling and identification of the dynamic response of a supported bridge, *Mechanical Systems and Signal Processing* 14 (1) (2000) 75–89.
[23] M.A. Mahmoud, M.A. Abouzaid, Dynamic response of a beam with a crack subject to a moving mass, *Journal of Sound and Vibration* 256 (4) (2002) 591–603.
[24] J.W. Lee, J.D. Kim, C.B. Yun, J.H. Yi, J.M. Shim, Health-monitoring method for bridges under ordinary traffic loadings, *Journal of Sound and Vibration* 257 (2) (2002) 247–264.

[25] C. Bilello, L.A. Bergman, Vibration of damaged beams under a moving mass: theory and experimental validation, *Journal of Sound and Vibration* 274 (2004) 567–582.
[26] X.Q. Zhu, S.S. Law, Wavelet-based crack identification of bridge beam from operational deflection time history, *International Journal of Solids and Structures* 43 (2006) 2299–2317.
[27] R.N. Jazar, in: *Vehicle Dynamics Theory and Application*, Springer, New York, 2008.
[28] Y.H. Lin, M.W. Trethewey, Finite element analysis of elastic beams subjected to moving dynamic loads, *Journal of Sound and Vibration* 136 (2) (1989) 323–342.
[29] G.L. Qian, S.N. Gu, J.S. Jiang, The dynamic behaviour and crack detection of a beam with a crack, *Journal of Sound and Vibration* 138 (2) (1990) 233–243.
[30] I. Daubechies, Ten lectures on wavelets. *CBMS-NSF Conference Series*, 61. SISAM, Philadelphia, PA, 1992.
[31] L. Deng, C.S. Cai, Identification of parameters of vehicles moving on bridges, *Engineering Structures* 31 (2009) 2474–2485.
[32] R.L. Carlson, An experimental study of the parametric excitation of a tensioned sheet with a crack-like opening, *Experimental Mechanics* 14 (1974) 52–458.
[33] P. Gudmundson, The dynamic behaviour of slender structures with cross-sectional cracks, *Journal of Mechanics Physics Solids* 31 (1983) 329–345.